doi:10.1246/cl.2011.372

Published on the web March 5, 2011

When Microbubble–Polyelectrolyte Complexes Overcharge: A Comparative Study Using Electrophoresis

Hiroshi Frusawa* and Masaichi Inoue
Center for Nanoscience and Nanotechnology, Soft Matter Laboratory, Kochi University of Technology, Tosa-Yamada, Kochi 782-8502

(Received January 7, 2011; CL-110021; E-mail: frusawa.hiroshi@kochi-tech.ac.jp)

We observed the charge reversal of microbubble–polyelectrolyte complexes using microscopic electrophoresis. The measured mobility of microbubbles with the addition of cationic poly(allylamine hydrochloride) exhibited unusual behaviors. The critical concentration of polyelectrolytes added for the charge reversal was not only weakly dependent on chain length but was also much larger than that of colloidal silica–polyelectrolyte complexes. We attribute the nonstoichiometric overcharging to the adsorption–desorption kinetics of hydroxy ions on the surface of genuine microbubbles.

Microbubbles (MBs), or colloidal bubbles with diameter ranging from 0.1 to 100 μm, are finding not only material applications as templates for fabricating microcapsules[1,2] but also many biomedical applications[3,4] including ultrasound contrast agents, targeted drug delivery, and gene therapy. While conventional techniques of creating micron- and submicron-bubbles have been based on sonication or high-shear emulsification, new technologies, such as inkjet printing and microfluidic processing have also been developed for controlling MB characteristics.[5] The MBs tend to leak into aqueous solutions due to a large Laplace pressure that drives bubble dissolution.[6] To increase the lifetime of individual bubbles, the gas core can be coated by a shell to slow down the gas diffusion, achieving stability that lasts for a few months.[1,2] The low gas permeability leads to an efficient trapping of encapsulated gas inside solutions, which is of great interest in terms of green-technological applications including components of fuel cells and even industrial food applications, such as flavor additives.

The shell may comprise a variety of materials, such as proteins, lipids, and nanoparticles.[2] In particular, cationic shells are useful for DNA vehicles in gene therapy because nucleic acids can electrostatically couple directly to the surface of MB capsules.[4] It has been demonstrated that ultrasound-targeted MB destruction enhances in vivo transfection in gene therapy.[4] However, the capacity of the MB surface for DNA must be further increased. Recent attention has been paid to a new class of polymer shells, polyelectrolyte multilayers (PEMs),[7,8] which have the potential advantage of increasing the stability as well as the overall loading capacity of MB surfaces due to the electrostatic sandwiching of DNA between cationic layers.[9,10]

The PEM-shelled MBs have been fabricated using a layer-by-layer method that sequentially deposits oppositely charged polymers onto the core material.[7–11] When forming the first polyelectrolyte layer, cationic polymers are usually attached on a substrate of the lipid or protein shell instead of direct deposition on a gas core.[7–10] Recently, pure PEM was prepared in a process that involves several steps, such as the introduction of CO_2 MBs.[11] These elaborate methods for fabricating PEM-coated MBs suggest that there is some difficulty in implementing the charge reversal of unmodified anionic MBs that adsorb hydroxy ions (OH^-) on the gas surfaces except for strongly acidic solutions.[12] If this is true, the underlying mechanism behind the extraordinary overcharging has yet to be fully understood. In this letter, we will use microscopic electrophoresis to determine the critical polymer concentration of the added polyelectrolytes at which the effective charge per MB–polyelectrolyte complex changes sign. We will then compare the critical density with the isoelectric point of silica particles (SPs) measured by the same experimental setup.

We used a MB generator (OM4-GP-040, Aura Tech) for the production of submicron air bubbles from deionized water. The MB solutions were in the pH range of 6.5 to 7.0. We added two different species of poly(allylamine hydrochloride) (PAH), long PAH (molecular weight (M_w) 56000, Sigma) and short PAH (M_w 15000, Sigma), after passing them through a 0.2-μm-pore-size filter (Minisart, Sartorius). The pHs of MB–PAH complex solutions were in the range of 7.2 to 7.8. We detected gas particles that undergo Brownian motion and electrophoresis at 20 °C via dark-field microscopy using a ζ-potential analyzer with a rectangular cell of 1-cm height, 0.75-mm depth, and 9-cm length equal to the electrode gap length (Zeecom, Microtech). We determined the mean hydrodynamic diameter of the observed Brownian particles to be about 400 nm via the Stokes–Einstein relation, which is in agreement with a previous result for the same kind of MBs.[13] We also counted the number of Brownian particles and evaluated the absolute value of number density using SPs (Sigma) of nominal diameter 1 μm as a reference. Video observations of migrating particles enable one to measure the individual velocities by tracking the particles, which has been referred to as microscopic electrophoresis. The inherent electrophoretic drift velocity was obtained from fitting the theoretical distribution for rectangular cells[14] to the measured velocity profile. For a comparative study of charge-reversal phenomena, we measured the electrophoretic velocity of the SPs as typical anionic colloids. While the SP solutions with a number density of $\rho_{sp} \fallingdotseq 1.7\,\mathrm{fmol\,L^{-1}}$ were stable with a pH of 7.0, the SP solutions with PAHs added had a pH range of 7.5 to 8.0.

We investigated the sign change of the electrophoretic mobility when long PAH is added. By analyzing the electrophoretic trajectories that were observed in the midplane of the rectangular cell, we obtained the data for Figure 1. This figure depicts the velocity histogram of 150 particles in which a positive velocity directly represents migration parallel to the electric field with the strength of $5.6\,\mathrm{V\,cm^{-1}}$. Figure 1 clearly shows that the measured velocity shifts from negative to positive while increasing the added concentration, C_L, of long PAH. We also find a broad velocity distribution in the absence of PAH,

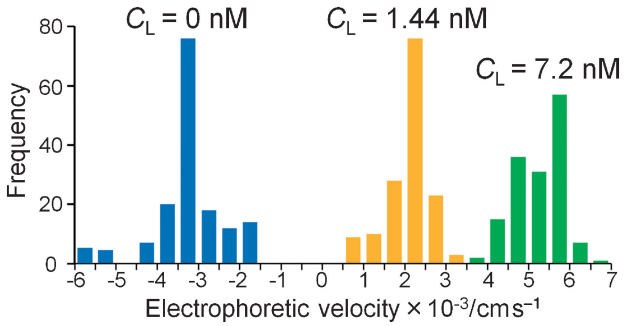

Figure 1. A comparison of the velocity distributions among microbubble solutions without adding PAH (blue), with 1.44 nM of PAH added (yellow), and with 7.2 nM of PAH added (green). These are measured velocities including the electroosmotic effect in the midplane of the rectangular cell.

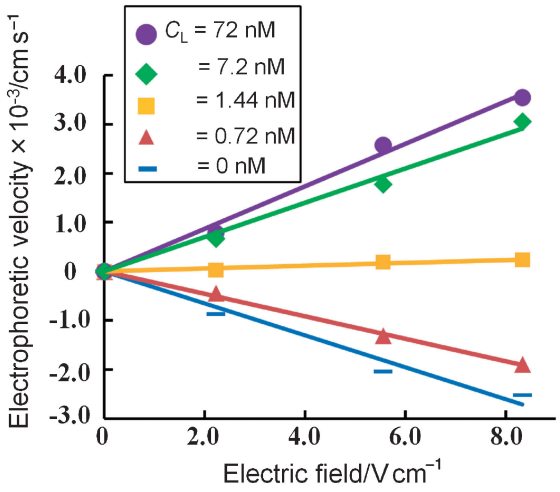

Figure 2. The data for each C_L can be represented by fitting straight lines of different slopes, which demonstrates a slope change in the graph of electrophoretic velocity vs. electric field. This reflects the change of effective charge per MB due to the addition of long PAH.

which is consistent with the previous study that reported a larger size dispersion of air MBs compared to the data for oxygen MBs.[13]

Figure 2 displays variations in the slope of the linear relationship between the applied electric field and the inherent electrophoretic mobility extracted from the analysis of the positionally dependent velocity as described before. As the long PAH density, C_L, is increased, the slope that is equal to the electrophoretic mobility increases, and the sign of the mobility is reversed beyond a critical PAH concentration C_L^*. In the absence of PAH, the obtained electrophoretic mobility yields a ζ potential of -47 mV, which is higher than that[13] for the same kind of bubbles at a pH of about 6.0 but is close to that[12] for micron bubbles at a similar pH of about 7.0. It is seen from Figures 1 and 2 that the electrophoretic mobility of MB–PAH complexes is positive but is negligible when long PAH with a polymer concentration of $C_L = 1.44$ nM is added, suggesting that $0.72\,\text{nM} < C_L^* < 1.44\,\text{nM}$. In this range, however, we encounter experimental difficulties.

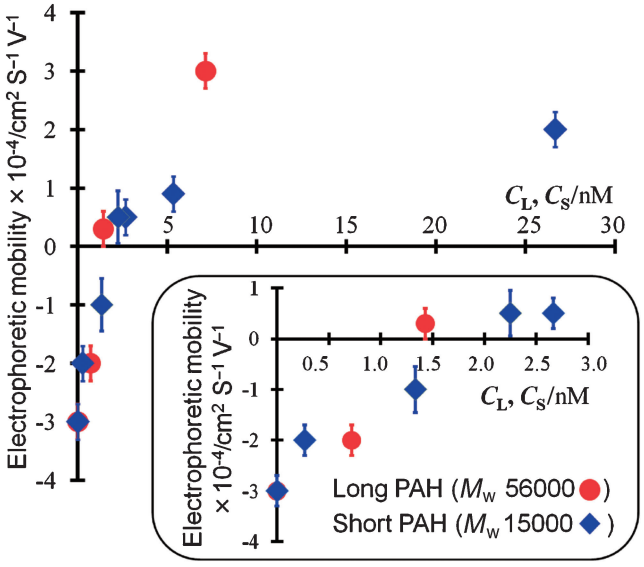

Figure 3. The electrophoretic mobilities as a function of added polymer concentration for long and short PAHs are plotted. Inset, magnified view. This finding shows that the mobility is reduced similarly, and the sign change of the mobility occurs at a similar polymer concentration regardless of the PAH chain length.

One is that cationic MBs undergoing electrophoresis in the opposite direction to that of genuine MBs coexist with apparently anionic MBs. The other is that even the apparently anionic MBs selected by microscopy observation have either negative or positive electrophoretic velocity after eliminating the electroosmotic contribution and rarely satisfy a linear relationship between electrophoretic velocity and electric field.

The microbubble density ρ_{mb} evaluated from counting the particle number in micrographs was independent of added polymer concentration C_L and was almost equal to the concentration ρ_{sp} of SPs for a few hours (Figure S1),[15] which was sufficient to finish electrophoretic measurements. It is also to be noted that the addition of PAHs as well as incubation time within a few hours hardly affects the mean hydrodynamic diameter evaluated by Brownian motions of MBs. The present stability even at $C_L = 1.44$ nM, the almost isoelectric point, is quite different from conventional colloidal phenomena. Conventional colloids have been found to induce a macroscopic phase separation due to the isoelectric colloid–polyelectrolyte complexation,[16] which reveals a specific state of the neutralized MB–PAH complexes. The unique overcharging of MBs will be discussed with the following comparative study.

Figure 3 depicts the dependence of electrophoretic mobility on polymer concentrations in both long and short PAHs, C_L and C_S. Before overcharging, the mobilities are reduced to a similar extent, and plausible data interpolations in the inset of Figure 3 provide the ranges of $0.72\,\text{nM} < C_L^* \leqq 1.4\,\text{nM}$ and $1.5\,\text{nM} \leqq C_S^* \leqq 2.2\,\text{nM}$. The close critical polymer concentrations indicate that the isoelectric point of MB–PAH complexes is not controlled by monomer density, contrary to the previous results of colloid–polyelectrolyte complexes.[17] In other words, different amounts of cationic charges that added polymers with different M_w carry are able to similarly neutralize the anionic MBs with the same charges.

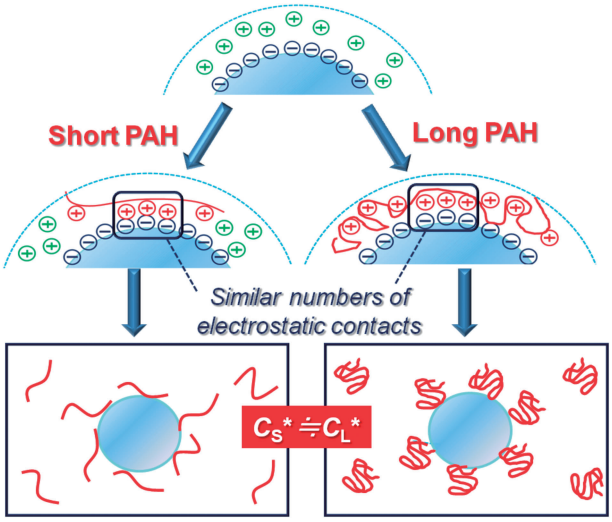

Figure 4. Schematic illustrations of charge-neutralized states due to the complexation of cationic polymers and MBs are depicted. We infer that dissociated polyelectrolyte charges participate in forming the electric double layer in the vicinity of a target microbubble while the number of attached charges per PAH is invariant with respect to the chain length.

For a more detailed comparison, we performed electrophoresis experiments of SPs with long PAH added and determined the critical polymer density D_c as a reference. Although we adjusted the number density, ρ_{sp}, of SPs to that of MBs ($\rho_{sp} = \rho_{mb}$) in measuring the electrophoresis, we obtained $D_c \fallingdotseq 0.04\,\mathrm{nM}$ for the SPs, which is much smaller than the above critical density for MBs: $18D_c < C_L^* \leqq 35D_c$. Assuming that the stoichiometry at the isoelectric point applies to the SP systems instead of MB solutions, we have an electrical neutrality relation, $Z_{sp}\rho_{sp} + Z_L C_L^* = 0$, with Z_{sp} and Z_L, respectively, being the valences per SP and long PAH. Consequently, we find that the surface charge density of SPs, σ_{sp}, is $\sigma_{sp} = -Z_{sp}e/(4\pi a^2) \fallingdotseq -5\mathrm{e\,nm^{-2}}$ where $a = 500\,\mathrm{nm}$ and e denotes the elementary charge. The present value ($|\sigma_{sp}|/e \fallingdotseq 5$) agrees with the number of silanol groups per $\mathrm{nm^2}$ reported in the literature.[18] The consistency of silica–polyelectrolyte complexes with the conventional stoichiometry[17] conversely makes it clear that the critical concentration C_L^* is far beyond the stoichiometric point, suggesting that MB–PAH complexes are surrounded by excess PAH even at the isoelectric point; the excess cationic polymers would interfere to form aggregates of the almost isoelectric MB–PAH complexes.

By focusing on the different nature of the surface charges between MBs and polymer colloids, we can now discuss the underlying mechanism behind the violation of the stoichiometry at the isoelectric points of MB–PAH complexes. While surface charges on polymer colloids are fixed with cores, the hydroxy ions temporarily attached on the surface of MBs are in adsorption equilibrium. Figure 4 is a schematic of the unique complexation state in MB–PAH mixtures that illustrates the following points. The number of neutralizing ionic groups per PAH should be weakly dependent on the PAH chain length because the initially attached cations of PAH may be dissociated from the MB surface nonelectrostatically due to desorption of hydroxy ions that occurs irrespectively of the presence of PAH chains. In this case, what is balanced with the gain of attractive electrostatic interaction energy in the weak adsorption equilibrium is thought to be the loss of translational entropy determined by surrounding polymer density, rather than the loss due to the configurational entropy.[19] Incidentally, the non-attached ionic groups on PAH can play a similar role to that of small counter ions located around the electric double layer, instead of directly neutralizing the hydroxy ions on the MB surface (see the middle illustrations in Figure 4). These discussions can explain why we obtained similar critical polymer concentrations irrespectively of polymer chain length.

In conclusion, we have unambiguously demonstrated using microscopic electrophoresis that the stoichiometry, which isoelectric colloid–polyelectrolyte complexes have strictly obeyed so far,[18] is violated for MB–PAH complexes. This finding indicates that electrostatic interactions play only a minor role in forming the first layer on genuine MBs compared to other factors such as the hydrophobicity of amphiphilic molecules. However, at the same time, Figure 3 shows that we are able to form PEMs without using additional materials or specific gases as long as the surplus of surrounding polyelectrolyte in forming the first layer is rinsed before depositing the second layer. Fundamentally, it is a challenging issue to develop a theory that reproduces the critical polymer concentration far beyond the stoichiometry. Such a theory would judge the validity of our view as illustrated in Figure 4.

This work was supported by the Yamada Science Foundation and KAKENHI, No. 19031027. We acknowledge T. Murakami and R. Yoshida for valuable help.

References and Notes

1 E. Dressaire, R. Bee, D. C. Bell, A. Lips, H. A. Stone, *Science* **2008**, *320*, 1198.
2 M. Borden, *Soft Matter* **2009**, *5*, 716.
3 S. R. Sirsi, M. A. Borden, *Bubble Sci., Eng. Technol.* **2009**, *1*, 3.
4 C. M. H. Newman, T. Bettinger, *Gene Ther.* **2007**, *14*, 465.
5 E. Stride, M. Edirisinghe, *Soft Matter* **2008**, *4*, 2350.
6 P. B. Duncan, D. Needham, *Langmuir* **2004**, *20*, 2567.
7 D. G. Shchukin, K. Köhler, H. Möhwald, G. B. Sukhorukov, *Angew. Chem., Int. Ed.* **2005**, *44*, 3310.
8 M. Winterhalter, A. F.-P. Sonnen, *Angew. Chem., Int. Ed.* **2006**, *45*, 2500.
9 I. Lentacker, B. G. De Geest, R. E. Vandenbroucke, L. Peeters, J. Demeester, S. C. De Smedt, N. N. Sanders, *Langmuir* **2006**, *22*, 7273.
10 M. A. Borden, C. F. Caskey, E. Little, R. J. Gillies, K. W. Ferrara, *Langmuir* **2007**, *23*, 9401.
11 H. Daiguji, E. Matsuoka, S. Muto, *Soft Matter* **2010**, *6*, 1892.
12 M. Takahashi, *J. Phys. Chem. B* **2005**, *109*, 21858.
13 F. Y. Ushikubo, T. Furukawa, R. Nakagawa, M. Enari, Y. Makino, Y. Kawagoe, T. Shiina, S. Oshita, *Colloids Surf., A* **2010**, *361*, 31.
14 T. Palberg, H. Versmold, *J. Phys. Chem.* **1989**, *93*, 5296.
15 Supporting Information is available electronically on the CSJ-Journal Web site, http://www.csj.jp/journals/chem-lett/index.html.
16 C. L. Cooper, P. L. Dubin, A. B. Kayitmazer, S. Turksen, *Curr. Opin. Colloid Interface Sci.* **2005**, *10*, 52.
17 a) E. Kokufuta, K. Takahashi, *Polymer* **1990**, *31*, 1177. b) T. Okubo, M. Suda, *J. Colloid Interface Sci.* **1999**, *213*, 565. c) A. Y. Grosberg, T. T. Nguyen, B. I. Shklovskii, *Rev. Mod. Phys.* **2002**, *74*, 329.
18 A. A. Christy, P. K. Egeberg, *Analyst* **2005**, *130*, 738, and references therein.
19 R. R. Netz, D. Andelman, *Phys. Rep.* **2003**, *380*, 1.

